

Nonlinear observers for parameter estimation in a solution polymerization process using infrared spectroscopy

N. Sheibat-Othman^{a,*}, D. Peycelon^b, S. Othman^a, J.M. Suau^b, G. Févotte^a

^a LAGEP-Université Lyon I-CNRS/ESCEPE, Bât 308, 43 Boulevard du 11 Nov. 1918, 69622 Villeurbanne cedex, France

^b Coatex ZI Lyon Nord, 69727 Genay, France

Received 4 October 2007; received in revised form 28 November 2007; accepted 29 November 2007

Abstract

Adaptive and high gain nonlinear observers are used for state and parameter estimation in an industrial polymerization process. The solution homopolymerization of acrylic acid is considered. The process is monitored online by near infrared spectroscopy giving the residual amount of monomer. Using this measurement, a continuous adaptive observer is first constructed to estimate the concentration of radicals. A second high gain continuous-discrete observer uses off-line measurements of the polymer molecular weight to estimate the termination rate coefficient that might be time varying due to the gel effect. The transfer to solvent rate coefficient is estimated under steady-state conditions and is assumed to be constant during the reaction. The identified model is validated by varying the process parameters: the concentrations of solvent, monomer, radicals and the residence time in the reactor with interest of their impact on the polymer molecular weight.
© 2007 Elsevier B.V. All rights reserved.

Keywords: Nonlinear continuous-discrete observer; Adaptive observer; Free radical polymerization; Molecular weight; Near infrared spectroscopy

1. Introduction

Polymerization processes are concerned by observer development for process monitoring, control, fault detection and isolation and for parameter estimation. In this work, we are interested in parameter and state estimation of a solution homopolymerization reaction using nonlinear observers.

Usually, for constant parameters, identification is done by fitting algorithms based on nonlinear optimisation [1,2] or using the sequential Monte Carlo method [3]. Arora and Biegler [4] presented a nice application of the trust-region nonlinear programming algorithm for parameter estimation of a polymerization model. For estimating time-varying model parameters or for state estimation, state observers are usually used. The extended Kalman filter (EKF) is still the most widely used [5–9]. However, different applications of nonlinear observers can now be found in polymerization processes due to the process nonlinearity and complexity [10–14].

The process underhand is monitored by near infrared (NIR) spectroscopy that is calibrated to estimate the residual amount

of monomer. Near infrared spectroscopy is now used in many industries for process monitoring. In homogeneous media, it is known to give chemical information about the reaction medium as long as the chemical functions have an impact in the near region. Many papers treated monitoring of the concentration of monomer in homogenous media [15–17]. The near spectra can also be affected by other properties such as the particle size in heterogeneous systems or by mechanical properties such as the polymer molecular weight. Such works are more recent and show limitations of this technique in many cases [18–21]. Therefore, for the moment, the polymer molecular weight should be measured by another technique or estimated from the process model. In this case, the parameters involved in the model should be identified. These parameters are mainly the transfer to solvent rate coefficient and the termination rate coefficient.

In this paper, we are interested in identifying the parameters involved in the model representing the evolution of the polymer molecular weight in order to be able to monitor it online. First of all, an estimation of the concentration of radicals is done using an adaptive observer based on the measurement of the concentration of monomer. Thereafter, the termination rate coefficient is estimated using a continuous-discrete observer based on off-line measurements of the polymer molecular weight. The observers are validated experimentally on a 30 L continuous industrial

* Corresponding author. Tel.: +33472431850; fax: +33472431699.
E-mail address: nida.othman@lagep.cpe.fr (N. Sheibat-Othman).

Nomenclature

k_p	propagation rate of monomer ($\text{cm}^3/\text{mol/s}$)
k_f	coefficient of transfer to solvent rate ($\text{cm}^3/\text{mol/s}$)
k_t	coefficient of radical termination rate ($\text{cm}^3/\text{mol/s}$)
M_n	instantaneous polymer number molecular weight (g/mol)
\bar{M}_n, \bar{M}_w	cumulative average number and weight molecular weights (g/mol)
MW_m	monomer molecular weight (g/mol)
N_m, N_s, N_i	residual number of moles of monomer, solvent and initiator (mol)
$F_m^{\text{in}}, F_s^{\text{in}}$	inlet molar flow rates of monomer and solvent (mol/s)
$F_m^{\text{out}}, F_s^{\text{out}}$	outlet molar flow rates of monomer and solvent (mol/s)
Q_i^{in}	volumetric inlet flow rate of component i (cm^3/s)
Q^{out}	total volumetric outlet flow rate (cm^3/s)
R_p, R_f	propagation and transfer rates (mol/s)
$[R^*]$	concentration of radicals (mol/cm^3)
V	total volume of the continuous reactor (cm^3)
λ_i	moments i of living polymer chains (mol/cm^3)
μ_i	moments i of dead polymer chains (mol/cm^3)

pilot reactor during the solution polymerization of acrylic acid. The identified model representing the evolution of the polymer molecular weight is validated under different process operating conditions. The concentrations of solvent, monomer, radicals and the residence time in the continuous reactor are varied in order to investigate the process.

2. Experimental setup

The free radical solution polymerization of acrylic acid is studied in this work. The reaction takes place in a 30 L jacketed well-mixed reactor equipped with internal reflux condenser. A Rushton turbine ensures the reactor homogeneity with a stirring rate of 150 rpm. Four positive-displacement gear pumps are used to feed the reactor with initiators, monomer and solvent. The flow rate of the pumps is measured using mass flowmeters. In the continuous process, the reactor overflows in a 250 L reactor where the residual monomer is consumed.

The reactants (monomer, solvent and initiator) are used without any purification. The reactor is initially charged with water and solvent (isopropyl alcohol) which plays the role of a chain transfer agent during the reaction. This charge is heated to 80°C using the jacket. The monomer and initiators are then introduced at fixed flow rates. Radicals are produced by a redox reaction. A reflux allows maintaining the reaction temperature around 80°C . Since the reaction is very exothermic, no heat is supplied to the reactor via the jacket once the reaction started. Also, no cooling is necessary, since the solvent is condensed continuously on the condenser which maintains the reaction temperature constant.

The NIR transmission probe is immersed in the 30 L reactor and is connected through fiber optics to a FOSS NIRSystems®

industrial spectrometer. The spectral data are acquired and processed online. The calibration models were developed and validated by Sheibat-Othman et al. [18]. The residual amount of acrylic acid is measured offline by high pressure liquid chromatography (HPLC) to validate the infrared predictions. An apparatus Agilent (1100 Series) was equipped with a column and precolumn of Waters Atlantis T3 C18 $3.5\ \mu\text{m}\ 4.6\ \text{mm} \times 50\ \text{mm}$ where a mobile phase of 95/05 water/methanol solution by volume (+1.8% phosphoric acid) circulates at a flow rate of $0.8\ \text{mL}\ \text{min}^{-1}$, at 30°C and under a pressure between 70 and 90 bars. The volume of an injection is $5\ \mu\text{L}$. The retention time of acrylic acid is 4.4 min. The whole analysis takes therefore 5 min. The acrylic acid is detected at 197 nm.

The polymer molecular weight distribution is measured by gel permeation chromatography (GPC). A GPC comprising a 515 Waters pump, one or two Ultrahydrogel Linear $7.8\ \text{mm} \times 30\ \text{cm}$ columns (mixed bed column with pore size ranging from 120 to $2000\ \text{\AA}$) with a guard precolumn and a 410 Waters refractometer was used. Elution was performed at 60°C ($0.5\ \text{ml}/\text{min}$) using an aqueous buffer ($\text{NaHCO}_3\ 0.05\ \text{M}$, $\text{NaNO}_3\ 0.1\ \text{M}$, triethanolamine $0.02\ \text{M}$, $\text{NaN}_3\ 0.03\%$). Calibration was relative to polyacrylic acid standards. GPC samples were neutralized with sodium hydroxide before injection in the GPC.

3. Process model

In solution polymerization, the monomer and polymer are soluble in the continuous phase that consists in this process of a water-solvent mixture. To write the process model, one has to consider the evolution of the concentrations of monomer and radicals in the reactor. The process model has also to describe the important polymer properties. In this application, the product quality is determined by the polymer molecular weight. The model describing the polymer molecular weight is therefore presented along with the material balances of the different reactants.

The material balance of monomer in a CSTR is given by the following equation:

$$\dot{N}_m = F_m^{\text{in}} - F_m^{\text{out}} - R_p = F_m^{\text{in}} - Q_{\text{out}} \frac{N_m}{V} - k_p N_m [R^*] \quad (1)$$

With N_m , the number of moles of residual monomer, F_m^{in} and F_m^{out} the input and output molar flow rates of monomer, Q_{out} the total volumetric output flow rate, k_p the propagation rate constant and $[R^*]$ the concentration of radicals in the reactor.

The solvent used plays the role of a chain transfer agent. It was found however by gas chromatography that the concentration of solvent is not importantly affected by the reactions of transfer. The material balance of solvent is therefore given by:

$$\begin{aligned} \frac{dN_s}{dt} &= F_s^{\text{in}} - F_s^{\text{out}} - R_f \\ &= F_s^{\text{in}} - Q_{\text{out}} \frac{N_s}{V} - \underbrace{k_f [R^*] N_s}_{\approx 0} \end{aligned} \quad (2)$$

The volume of the reaction medium is therefore:

$$\frac{dV}{dt} = \sum_i Q_i^{\text{in}} - Q^{\text{out}} \quad (3)$$

where Q_i^{in} is the volumetric flow rate of component i entering the reactor.

The concentration of radicals can be calculated from the amount of initiator introduced to the reactor if the initiator decomposition and termination reaction coefficients are known. One has to keep in mind, however, that these reactions are sensitive to impurities. Also, the reaction coefficients are temperature dependent and the termination rate coefficient might also be diffusion controlled depending on the concentration of polymer. For these reasons, we will be interested in estimating the concentration of radicals online. The model developed here will not involve the material balance of initiator that has not to be identified and there is no need to provide the model with the type and amount of initiator used.

The polymer molecular weight distribution can be described by the method of moments. Due to the small length of the formed chains during the reaction, only termination by dissociation is supposed to take place. The combination term is neglected. Applying the steady-state hypothesis to the balances of living polymer chains (radicals) of the three first moments gives (for more details see [22]):

$$\begin{aligned} \lambda_0 &= [R^*] \\ \lambda_1 &= \frac{k_t \lambda_0 + k_p N_m / V + k_f N_s / V}{k_t \lambda_0 + k_f N_s / V} \lambda_0 \\ \lambda_2 &= \left(1 + \frac{2k_p N_m / V}{k_t \lambda_0 + k_f N_s / V} \right) \lambda_1 \end{aligned} \quad (4)$$

Where N_s is the number of moles of chain transfer agent in the reactor, k_t the termination rate coefficient and k_f is the coefficient of the rate of transfer to the chain transfer agent.

The first three moments of dead polymer chains are given by the following differential equations:

$$\begin{aligned} \dot{\mu}_0 &= \frac{k_t \lambda_0^2 + k_f \lambda_0 N_s}{V} \\ \dot{\mu}_1 &= \frac{k_t \lambda_0 \lambda_1 + k_f \lambda_1 N_s}{V} \\ \dot{\mu}_2 &= \frac{k_t \lambda_0 \lambda_2 + k_f \lambda_2 N_s}{V} \end{aligned} \quad (5)$$

These moments allow calculating the polymer molecular weight. The cumulated average number molecular weight requires the calculation of only the first two moments of living and dead polymer chains:

$$\bar{M}_n = MW \frac{\mu_1 + \lambda_1}{\mu_0 + \lambda_0} \cong MW_m \frac{\mu_1}{\mu_0} \quad (6)$$

The instantaneous average number molecular weight is given by:

$$M_n = MW_m \frac{d\mu_1/dt}{d\mu_0/dt} \quad (7)$$

where MW_m is the molecular weight of monomer.

In order to obtain an online estimate of the polymer molecular weight, the parameters k_f and k_t have to be estimated. One has also to have an estimate of the concentration of radicals during the reaction. First of all, we consider the estimation of the concentration of radicals in the reactor $[R^*]$ (or λ_0). Afterwards, we study the estimation of the parameters k_f and k_t .

4. Estimation of λ_0

To estimate the concentration of radicals in the reactor, we consider the following augmented system:

$$\begin{aligned} \underbrace{\begin{bmatrix} \dot{N}_m \\ \dot{\lambda}_0 \end{bmatrix}}_x &= \underbrace{\begin{bmatrix} 0 & -k_p N_m \\ 0 & 0 \end{bmatrix}}_{A(y)} \begin{bmatrix} N_m \\ \lambda_0 \end{bmatrix} \\ &+ \begin{bmatrix} F_m^{\text{in}} - Q^{\text{out}} \frac{N_m}{V} \\ 0 \end{bmatrix} + \begin{bmatrix} 0 \\ \varepsilon_{\lambda_0} \end{bmatrix} \\ y &= \underbrace{\begin{bmatrix} 1 & 0 \end{bmatrix}}_C \begin{bmatrix} N_m \\ \lambda_0 \end{bmatrix} \end{aligned} \quad (8)$$

where ε_{λ_0} represents the unknown dynamic of λ_0 and y the measured output. Writing the system under this form allows determining the class of systems to which it belongs and therefore to determine which observer is the best adapted. It should be reminded that, in free-radical polymerization, the quasi-stationary hypothesis is usually applied to λ_0 . Writing system 8 does not contradict this assumption.

System 8 shows that λ_0 is observable whenever N_m is different from zero. A high gain observer can be constructed to estimate λ_0 . Also note that λ_0 attains quickly a stationary state. This state can therefore be considered as a parameter that is constant on small intervals or that is varying slightly. Therefore, also an adaptive observer can be used to estimate λ_0 [23]. The interest of the adaptive observer in this case is that regulation of the parameter observer is different from that of the state which allows a better tuning of the observer in order to have a rapid convergence without high sensitivity to measurement noise.

The adaptive observer of λ_0 takes the following form:

$$\begin{aligned} \dot{\hat{N}}_m &= F_m^{\text{in}} - Q^{\text{out}} N_m / V - k_p N_m \hat{\lambda}_0 - (\theta \kappa + \hat{\Gamma}^2)(\hat{N}_m - N_m) \\ \dot{\hat{\lambda}}_0 &= \theta \hat{\Gamma}(\hat{N}_m - N_m) \\ \dot{\hat{\Gamma}} &= -\theta(\kappa \hat{\Gamma} + k_p N_m) \end{aligned} \quad (9)$$

where θ and κ are the tuning parameter of the observer.

In order to validate the observer experimentally, its performance is first compared to the value of λ_0 calculated by deriving N_m in Eq. (1) and then to three other observers: the high gain observer [14], the EKF [5–9] and a minimization based observer over a receding horizon [24]. In this experiment, N_m was measured by NIR spectroscopy. All observers' results were less oscillating than the value obtained by deriving N . One should, however, be careful when comparing the behaviors of these observers that depend on their tuning. Fig. 1 shows that all observers converge to the real N_m and give simi-

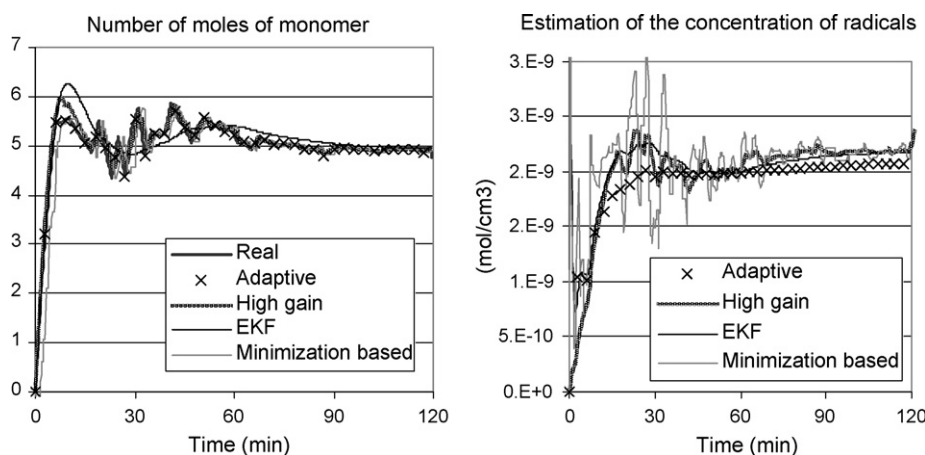


Fig. 1. Estimation of N_m and λ_0 during the semi-batch experiment SB1 using 4 observers: adaptive, high gain, extended Kalman filter and a minimization based observer.

lar estimations of λ_0 and therefore all observers can be used for this process. Oscillations in the minimization based observer depend on the horizon length, taken 90 s in this simulation. Longer horizons gave a static error at the beginning but were less oscillating afterwards. An evolution of the horizon length with time would probably improve the results. The run times of these observers for this simulation were: 0.19, 4.4, 54.8 and 384 s for the high gain, EKF, adaptive and the minimization based observer, respectively. The run times of the first three observers depend on the values of the tuning parameters and the run time of the minimization based observer depends on the method of optimization (lsqnonlin of Matlab[®]) that can surely be reduced with a well adapted method and on the horizon length. A difficulty was encountered when applying the EKF since when applying it to a different experiment its tuning had to be slightly adapted (the initial values of the covariance matrix). The high gain observer was the easiest to tune since it has only one tuning parameter. However, the adaptive observer allowed us to give a different rate of convergence to the state N_m than to the parameter λ_0 by tuning the parameters κ and θ which is interesting in presence of measurement noise to avoid oscillations in the parameter estimation. The adaptive observer will be used in the remainder of the paper.

5. Parameter estimation

The estimation of λ_0 does not necessitate the knowledge of the parameters k_f and k_t . Identification of these parameters is therefore decoupled from the estimator of λ_0 that can therefore be used in the procedure of identification of these parameters.

The sensitivity analysis has shown that the simultaneous identification of the parameters k_f and k_t was not possible. Variations in the parameter k_t affect much less the output than the parameter k_f . The parameters k_t and k_f has to be identified separately. Based on the free volume theory (see for instance [2]), k_t might vary during the reaction. Thus, one cannot simply try to remove the solvent and estimate the termination rate coefficient since

this last one is a function of the concentration of solvent in the reactor. Very high polymer chains were obtained when the reaction was realized without solvent (increasing exponentially from 4000 to 10,000 g/mol during the reaction).

Therefore, k_f is first calculated under steady-state conditions and k_t is then estimated during the reaction. It is important to mention, however, that k_f has to be updated if important variation in the operating conditions is considered, mainly temperature.

5.1. Estimation of the parameter k_f

The parameter k_f is identified based on the results of two continuous experiments where the same flow rates of initiator and monomer are employed during the continuous part but different flow rates of solvent. Under steady-state conditions, the instantaneous molecular weight is equal to the cumulative one.

The concentration of monomer is monitored by NIR spectroscopy as shown on Fig. 2. Real values of the concentration of monomer in the reactor are obtained by HPLC. The concentration of radicals is then estimated from the material balance by the adaptive observer presented in Eq. (9). \bar{M}_n is measured offline by GPC, V is constant and N_s is calculated from Eq. (2) using the different flow rates.

Identification of k_f is done at a moment during the stationary state (about 400 min) using Eq. (7). For $k_p = 1e^6 \text{ cm}^3/\text{mol/s}$, we obtain $k_f = 1300 \text{ cm}^3/\text{mol/s}$.

5.2. Estimation of the parameter k_t

Since k_t is susceptible to change during the reaction, it cannot be obtained by the fixed fitting algorithm. A sliding horizon optimization should be considered or a continuous-discrete observer since continuous measurements of N_m are obtained online by the NIR spectrometer and discrete measurements of \bar{M}_n are obtained offline by GPC. An application of such observers to polymerization reactions was proposed by Astorga et al. [25].

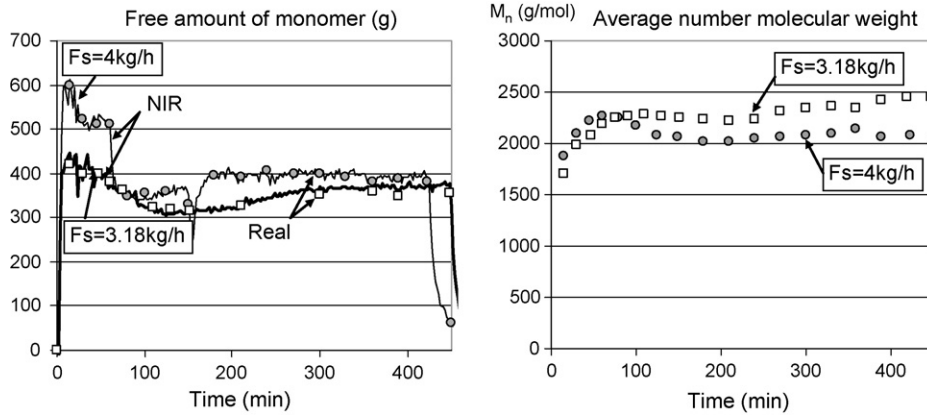


Fig. 2. Two continuous experiments with different flow rates of solvent for the identification of k_f (C1 $F_s^{in} = 3.18 \text{ kg/h}$ and C3 $F_s^{in} = 4 \text{ kg/h}$). The real amount of monomer is obtained by HPLC and M_n by GPC.

The following system is considered for the estimation of k_t :

$$\begin{cases} \frac{d\mu_0}{dt} = \frac{k_t \lambda_0^2 + k_f \lambda_0 N_s}{V} \\ \frac{dk_t}{dt} = 0 \\ y = \bar{M}_n = MW \frac{\mu_1}{\mu_0} \end{cases} \quad (10)$$

A change of coordinates is necessary in order to put the system under a canonical form of observability:

$$\begin{bmatrix} \phi_1 \\ \phi_2 \end{bmatrix} = \begin{bmatrix} y \\ L_f y \end{bmatrix} = \begin{bmatrix} \bar{M}_n \\ -\frac{MW\mu_1}{\mu_0^2} (k_t \lambda_0^2 + k_f N_s \lambda_0 / V) \end{bmatrix} \quad (11)$$

The continuous-discrete form of the high gain observer applied to system (11) is divided into two parts: a part of prediction and a part of correction. The prediction on the interval $t \in [t_k, t_{k+1}]$ is represented by:

$$\begin{cases} \dot{\hat{\mu}}_0 = \frac{k_t \lambda_0^2 + \hat{k}_t \lambda_0 N_s}{V} \\ \dot{\hat{k}}_t = 0 \\ \dot{S}(t) = -\theta S(t) - A^T S(t) - S(t)A \end{cases} \quad (12)$$

The correction at time $t = t_{k+1}$ is represented by:

$$\begin{bmatrix} \hat{\mu}_0(t_{k+1}) \\ \hat{k}_t(t_{k+1}) \end{bmatrix} = \begin{bmatrix} \hat{\mu}_0 \\ \hat{k}_t \end{bmatrix}_{t_{k+1}^-} - \kappa \begin{bmatrix} \frac{\partial \phi_1}{\partial \mu_0} & 0 \\ \frac{\partial \phi_2}{\partial \mu_0} & \frac{\partial \phi_2}{\partial k_t} \end{bmatrix}^{-1} \Big|_{t_{k+1}^-} S^{-1} |_{t_{k+1}} C^T (\hat{\mu}_0 |_{t_{k+1}^-} - \mu_0 |_{t_{k+1}}) \quad (13)$$

$$S(t_{k+1}) = S(t_{k+1}^-) + T_e C^T C$$

where θ and κ are two tuning parameters and T_e represent the sampling time period.

Simulation of the observer is shown on Fig. 3 that shows the estimated k_t and \bar{M}_n . A measurement of the polymer average number molecular weight was considered every 20 min. It can be seen that the observer converges by steps at each correction. It is worthy to mention that while estimating the parameter k_t in simulation, at higher values of k_f , k_t becomes non-observable. In this case, k_t can simply be neglected in the model of the molecular weight.

Three semi-batch experiments were then realized to identify k_t experimentally (Table 1) since in continuous experiments k_t is not supposed to vary. Fig. 4 shows the results of the observer while applied to these experiments. In all experiments, k_t was initialized at $4e^{-9}$. This value was approximated from the value

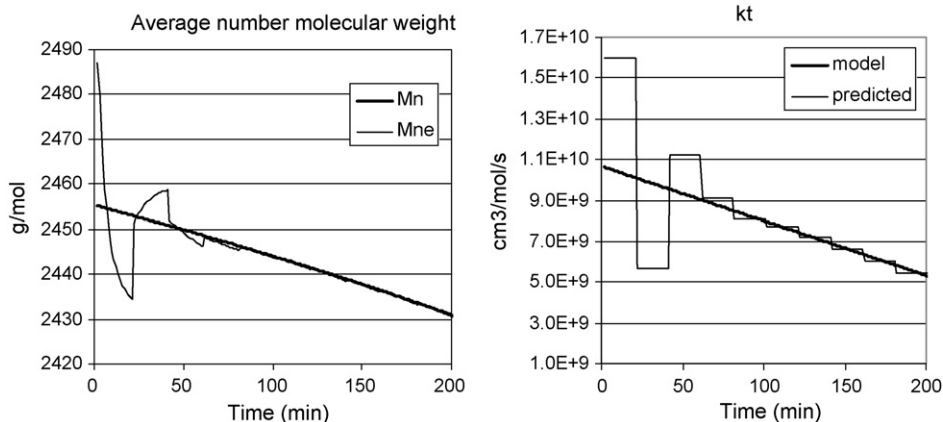


Fig. 3. Simulation of the continuous-discrete observer of k_t .

Table 1
Semi-batch experiments for the estimation of k_t

Experiment	Operating conditions
SB1	Q_I (initiator flow rate) = 0.68 kg/h, monomer addition time $T_f = 120$ min. No monomer in the initial charge of the reactor
SB2	$Q_I = 0.75$ kg/h, $T_f = 120$ min. No monomer in the initial charge
SB3	$Q_I = 0.68$ kg/h, $T_f = 90$ min with 4% of monomer in the initial charge

obtained under steady-state conditions assuming that a higher value is necessary at the beginning since the concentration of polymer is still low. It is worthy to mention that initializing k_t far from the optimal values is not favorable with such measurement intervals of \bar{M}_n (20 min). It should be mentioned also that the observer of k_t is based on that of λ_0 . Therefore, the second observer would not converge until the first one converges. Initial estimations of k_t are therefore suspicious until few measurements are available to ensure the convergence of both observers especially if k_t is initialized far from the real value. It can be seen that in all experiments, the observer converges to the same profile. The variation of k_t with the concentration of polymer can be identified for the use in the model of \bar{M}_n . A linear relation could be obtained such that: $k_t = k_{t0} + b \times SC$, with $k_{t0} = 4 \times 10^9$, $b = -0.98 \times 10^8$ and SC is the solids content in %.

In order to provide evidence of a varying k_t , Fig. 5 compares the polymer molecular weight obtained by the continuous-discrete observer and the open-loop model with a constant k_t . It can be seen that the increase of the polymer molecular weight is conditioned by a decrease in k_t in view of the concentrations of the different components.

It was found from these experiments that tuning the continuous-discrete observer was very important in order to obtain a rapid convergence to the real values. This is due to the fact that the observer is based on a small number of measurements and on the cumulative not instantaneous polymer molecular weight. It was found that a best comportment of the observer was obtained with small values of θ and high values of κ .

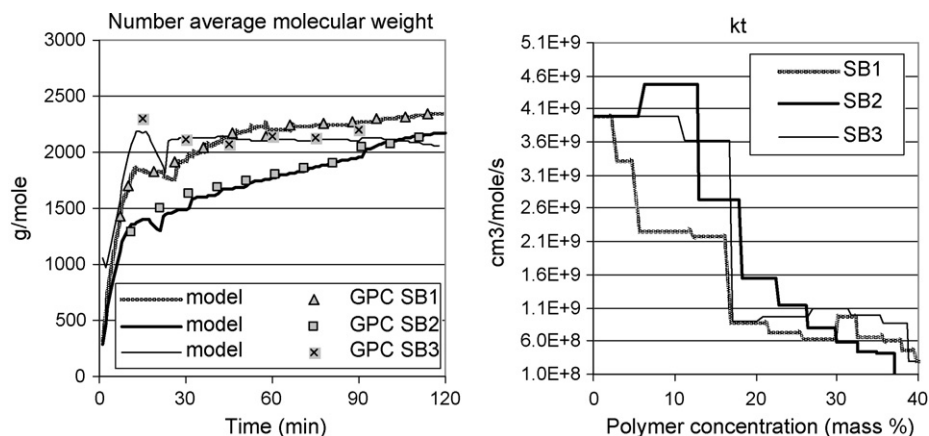


Fig. 4. Application of the continuous-discrete observer of k_t to the semi-batch experiments (SB1, SB2, SB3, Table 1).

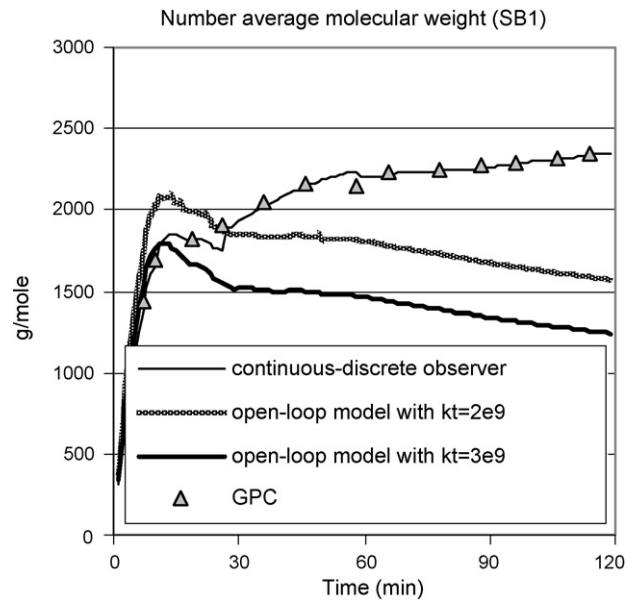


Fig. 5. Estimation of the polymer molecular weight using the open-loop model with constant k_t (SB1).

6. Investigation of the continuous process

The identified model is validated by varying the operating conditions in the continuous process. The influence of the concentrations of monomer, radicals and solvent and the residence time in the reactor on the polymer molecular weight is studied (Table 2).

6.1. Influence of the concentration of solvent

The influence of the solvent concentration in the continuous part was studied in experiments C2 and C3 where the solvent to monomer mass ratio was 58.36 and 87.49, respectively. Experiment C3 contains therefore 35% more solvent than C2. The continuous part of the reaction starts when the 30 L reactor is full and overflows into a 250 L reactor. This takes place at 60 min in experiment C3 and at 90 min in experiment C2 due to the difference in the total input flow rate. Also, the initial charge of

Table 2

Continuous experiments to study the influence of the operating conditions on the polymer molecular weight

Operating conditions	Experiment				
	C1	C2	C3	C4	C5
Total flow rate (kg/h)	13.9	14.13	14.1	13.9	20
Monomer (%)	40.04	39.7	32.46	33.07	40.04
Initiator/monomer ($I/M \times 100$) (diluted initiator solution)	27	26.74	27.48	21.77	27
Solvent/monomer ($S/M \times 100$)	57.27	58.36	87.49	87.54	57.26
\bar{M}_n (g/mol)	2400	2300	2000	2400	2680

both reactions was not identical. More solvent was introduced in the initial charge of experiment C3.

Fig. 6 shows a comparison between these experiments. The evolution of the concentration of free monomer in the reactor is obtained by the NIR spectrometer and validated by HPLC. During the continuous part, the amount of residual monomer reaches the same value in both experiments. This shows that, as expected, the concentration of solvent has no influence on the reaction rate. An estimation of the solids contents in both reactions C3 and C2 is also obtained by the NIR spectrometer and validated by gravimetry. The difference in the solids content between the experiments is due to the change in the solvent to monomer ratio.

The figure shows that the concentration of radicals decreases while increasing the concentration of solvent. On one hand, this

can be due to a best solubility of the initiator in a mixture with more water. On the other hand, a higher termination rate coefficient is expected in a process with more solvent due to a best mobility of radicals which contributes to decreasing the concentration of radicals. The decrease of the concentration of radicals as a function of the concentration of solvent contributes to an increase in the polymer molecular weight. However, increasing the concentration of solvent that plays a role of chain transfer agent contributes to a decrease in the polymer molecular weight. The resulting effect on the polymer molecular weight was negative as shows the figure. Increasing the solvent by 35% decreases the molecular weight by 17%. The identified model is in agreement with the experimental data. The estimation error at the very beginning is probably due to the convergence time of the observer of λ_0 .

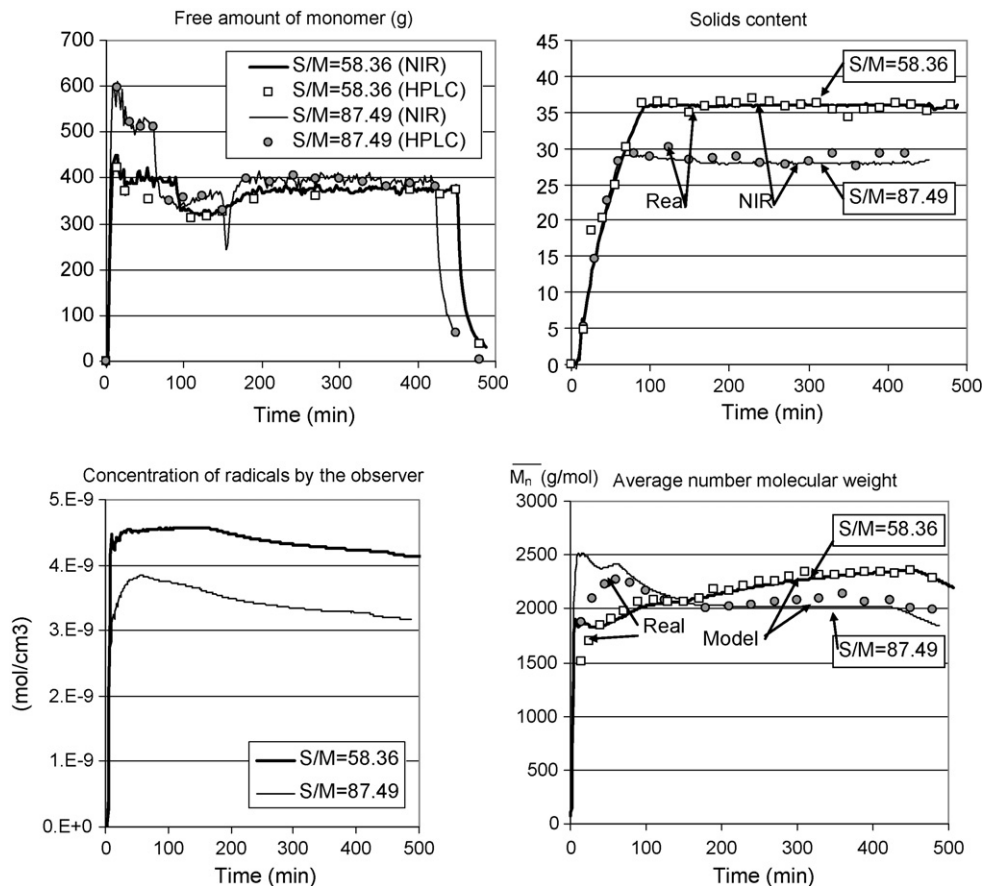


Fig. 6. Influence of the solvent to monomer mass ratio on the polymer molecular weight ($S/M = 58.36$ in C2 and 87.49 in C3 (+35% solvent)).

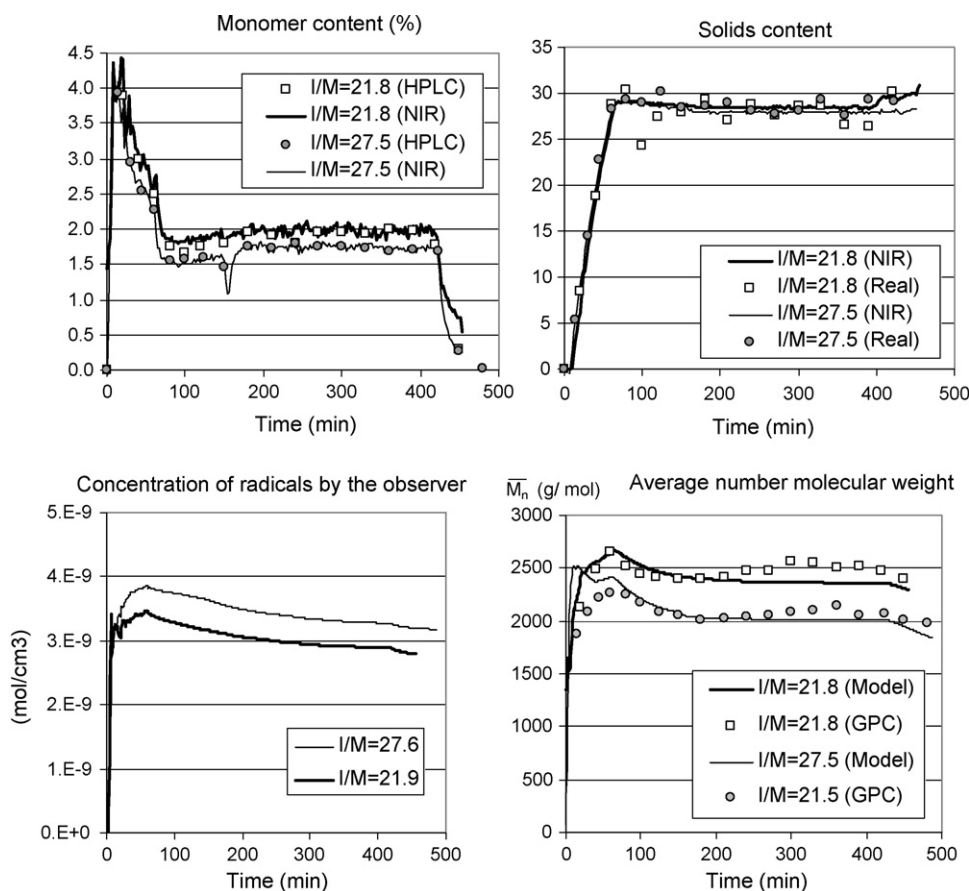


Fig. 7. Influence of the initiator to monomer mass ratio on the polymer molecular weight ($I/M = 27.5\%$ in C3 and 21.8% in C4 (-20% initiator)).

6.2. Influence of the concentration of initiator

In experiments C3 and C4, all the concentrations were maintained identical except for the initiator concentration where -20% of initiator was employed in experiment C4. The initiator to monomer concentration was therefore $(I/M) = 27.5\%$ in C3 and 21.8% in C4. Fig. 7 shows the radical concentration estimated in both experiments. A slight influence on the concentration of radicals is detected but this suffices to affect the reaction rate and therefore the residual amount of monomer. The figure clearly shows that the difference between both experiments is constant during the continuous part. A slight affect on the solids content is observed when changing the initiator concentration due to the change in the residual amount of monomer.

The polymer molecular weight is supposed to increase due to two factors. On one hand, it is affected by the concentration of radicals. The termination rate is increased and therefore the polymer molecular weight decreases. On the other hand, the concentration of monomer is decreased by increasing the initiator concentration. This contributes to the decrease in the polymer molecular weight according to Eq. (4). The figure shows that the change in the concentration of radicals altered importantly the polymer molecular weight while a slight change in the concentration of monomer was observed. Therefore, the polymer molecular weight is not only a function of the monomer con-

centration. This confirms that the termination phenomenon is not negligible in this application.

6.3. Influence of the residence time in the reactor

Experiments C2 and C5 were started with the same conditions. When the reactor started overflowing, different total flow rates (14 and 20 kg/h, respectively), but with identical concentrations, were applied. The ratios of monomer to solvent and to initiator were identical in both experiments.

Fig. 8 shows the results of these experiments. It can be seen that the residence time in the reactor influences importantly the concentrations of monomer and radicals in the reactor, which influences the reaction rate. The more the monomer remains in the reactor the more it is consumed which increases the overall conversion. The concentration of radicals decreases with the residence time. The solids content of the reactor is not influenced by the overall flow rate. As a result, the polymer molecular weight was importantly influenced by the residence time in the reactor. Increasing the residence time produces shorter polymer chains. The identified model predicted the evolution of the polymer molecular weight precisely in these experiments.

Increasing the overall flow rate of the reactor is interesting to minimize the process time. This point should however be studied carefully in order to ensure the final product quality. While increasing the overall flow rate, the concentrations of initiator

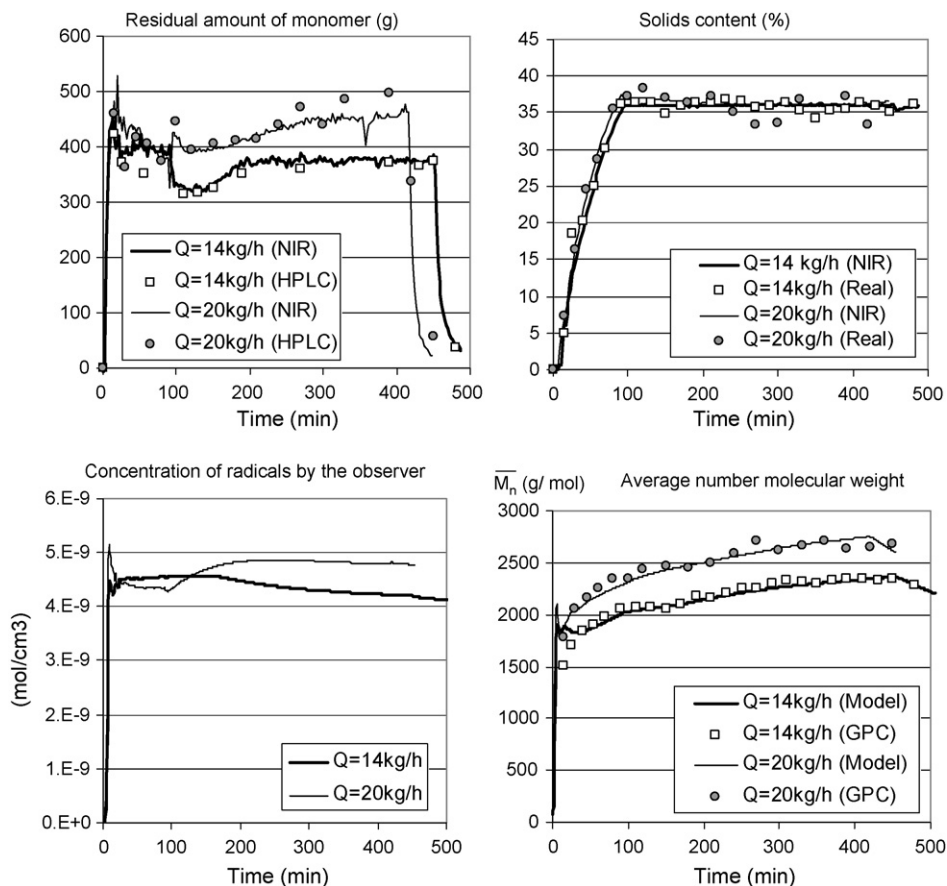


Fig. 8. Influence of the residence time on the polymer molecular weight (total flow rate $Q = 14$ kg/h in C2 and $Q = 20$ kg/h in C5, respectively).

or solvent should be corrected in order to avoid a decrease in the polymer molecular weight.

7. Conclusion

This work presents an application of nonlinear observers in polymerization processes. The adaptive observer was used to estimate the concentration of radicals and a high gain continuous-discrete nonlinear observer to estimate the termination rate coefficient. A slightly decreasing profile of k_t was detected as a function of the polymer concentration that is therefore diffusion controlled. The estimation strategy remains however valid for constant profiles of k_t . A model could be derived from this estimation to predict the variation of k_t with the concentration of polymer and to estimate the polymer molecular weight online.

The interest of these observers is that they do not need to have information about the initiator type or concentration nor on the model relating k_t to the concentration of polymer. The concentration of radicals is estimated from the reaction rate which allows taking into account the reaction temperature and the presence of impurities. The same argument applies for k_t .

However, the observers form a cascade where the convergence of the second one is conditioned by the convergence of the first one. Also, since the second observer is based on the cumulative molecular weight, it should be initialized close to the

real value. Any error done at the very beginning would affect the estimations for a period of time. For a correct initialization, one can use values obtained under steady-state conditions.

In polymerization reactions monitoring of the reaction rate and polymer molecular weight are primordial. Changes in the evolution of the process could be detected precisely and early using the model as the NIR spectrometer was difficult to calibrate for the polymer molecular weight. However, the NIR spectrometer gave very accurate results for the residual amount of monomer and polymer.

References

- [1] J.M. Asua, M.E. Adams, E.D. Sudol, A new approach for the estimation of kinetic parameters in emulsion polymerization systems. I. Homopolymerization under zero-one conditions, *J. Appl. Polym. Sci.* 39 (1990) 1183–1213.
- [2] T. De Roo, J. Wieme, G.J. Heyndrickx, G.B. Marin, Estimation of intrinsic rate coefficients in vinyl chloride suspension polymerization, *Polymer* 46 (2005) 8340–8354.
- [3] T. Chen, J. Morris, E. Martin, Particle filters for state and parameter estimation in batch processes, *J. Process Contr.* 15 (2005) 665–673.
- [4] N. Arora, L. Biegler, Parameter estimation for a polymerization reactor model with a composite-step trust-region NLP algorithm, *Ind. Eng. Chem. Res.* 43 (2004) 3616–3631.
- [5] J. Dimitratos, C. Georgakakis, M. El-Aassar, A. Klein, An experimental study of adaptive Kalman filtering in emulsion copolymerization, *Chem. Eng. Sci.* 46 (12) (1991) 3203–3218.

- [6] Z.L. Wang, F. Pla, J.P. Corriou, Nonlinear adaptive control of batch styrene polymerization, *Chem. Eng. Sci.* 50 (13) (1995) 2081–2091.
- [7] C. Scali, M. Morretta, D. Semino, Control of the quality of polymer products in continuous reactors: comparison of performance of state estimators with and without updating of parameters, *J. Process Contr.* 7 (5) (1997) 357–369.
- [8] C. Kiparissides, P. Sefelis, G. Mourikas, A.J. Morris, Online optimization control of molecular weight properties in batch free-radical polymerization reactors, *Ind. Eng. Chem. Res.* 41 (2002) 6120–6131.
- [9] M.J. Park, S.M. Hur, H.K. Rhee, Online estimation and control of polymer quality in a copolymerization reactor, *AIChE J.* 48 (5) (2002) 1013–1021.
- [10] M. Van Dootingh, F. Viel, D. Rakotopara, J.P. Gauthier, P. Hobbes, Nonlinear deterministic observer for state estimation: application to a continuous free radical polymerization reactor, *Comput. Chem. Eng.* 16 (8) (1992) 777–791.
- [11] M. Soroush, Nonlinear state-observer design with application to reactors, *Chem. Eng. Sci.* 52 (3) (1997) 387–404.
- [12] H. Hammouri, T.F. McKenna, S. Othman, Applications of nonlinear observers and control: improving productivity and control of free radical solution copolymerization, *Ind. Eng. Chem. Res.* 38 (1999) 4815–4824.
- [13] J. Alvarez, T. Lopez, Robust dynamic state estimation of nonlinear plants, *AIChE J.* 45 (1) (1999) 107–122.
- [14] N. Sh'eibat-Othman, G. Févotte, T. McKenna, Biobjective control of emulsion polymerizations: control of the polymer composition and the concentration of monomer in the polymer particles, *Chem. Eng. J.* 98 (1-2) (2004) 69–79.
- [15] A. Cherfi, G. Févotte, Online conversion monitoring of the solution polymerization of methyl methacrylate using near-infrared spectroscopy, *Macromol. Chem. Phys.* 203 (9) (2002) 1188–1193.
- [16] J.M.R. Fontoura, A.F. Santos, F.M. Silva, M.K. Lenzi, E.L. Lima, J.C. Pinto, Monitoring and control of styrene solution polymerization using NIR spectroscopy, *J. Appl. Polym. Sci.* 90 (5) (2003) 1273–1289.
- [17] V. Drcos, S. Monge, D. Haddleton, In situ Fourier transform near infrared spectroscopy monitoring of copper mediated living radical polymerization, *J. Polym. Sci: Polym. Chem.* 42 (2004) 4933–4940.
- [18] N. Sheibat-Othman, D. Peycelon, J.B. Egraz, J.M. Suau, G. Févotte, Control of the polymer molecular weight using near infrared spectroscopy, *AIChE J.* 50 (3) (2004) 654–664.
- [19] P.A.M. Steeman, A.A. Dias, D. Wienke, T. Zwartkruis, Polymerization and network formation of UV-curable systems monitored by hyphenated real-time dynamic mechanical analysis and near infrared spectroscopy, *Macromolecules* 37 (2004) 7001–7007.
- [20] E.S. Nogueira, C.P. Borges, J.C. Pinto, IN-line monitoring and control of conversion and weight-average molecular weight of polyurethanes in solution step-growth polymerization based on near infrared spectroscopy and torqueometry, *Macromol. Mater. Eng.* 290 (2005) 272–282.
- [21] I. Alig, P.A.M. Steeman, D. Lellinger, A.A. Dias, D. Wienke, Polymerization and network formation of UV-Curable materials monitored by hyphenated real-time ultrasound reflectometry and near infrared spectroscopy (RT-US/NIRS), *Prog. Org. Coat.* 55 (2006) 88–96.
- [22] J.S. Chang, P.H. Liao, Molecular weight control of a batch polymerization reactor: experimental study, *Ind. Eng. Chem. Res.* 38 (1999) 114–153.
- [23] Q. Zhang, Adaptive observer for MIMO linear time-varying systems, *IEEE T. Automat. Contr.* 47 (3) (2002) 525–529.
- [24] G. Zimmer, State observation by on-line minimization, *Int. J. Control* 60 (1994) 595–606.
- [25] C.M. Astorga, N. Othman, S. Othman, H. Hammouri, T.F. McKenna, Nonlinear continuous-discrete observers. Applications to emulsion polymerization reactors, *Control Eng. Pract.* 10 (1) (2002) 3–13.